14/20 joints on each side. To protect the system, the stopcock joint farthest from the NMR tube was closed with a serum cap. Neopentyllithium (0.01 g, 13 mmol) was weighed into the NMR tube in the dry box (Vaccuum Atmospheres) under an argon atmosphere. The NMR tube was closed with the stopcock assembly, removed from the drybox, and cooled to -78 °C with dry ice-propanol. Meanwhile TMEDA, distilled from CaH_2 (0.03 g), was weighed in the drybox and dissolved in THF-d_8 (distilled from Na-K) (0.440 g). This mixture was drawn into a glass syringe, protected by a three-way luer valve with a septum blocking the side opening of the valve (the latter was closed to the syringe side), and dry argon was blown through the needle to remove traces of air. Then the needle was drawn through the protecting serum cap through the stopcock and as far as possible into the cooled NMR tube. The THF-TMEDA mixture was slowly syringed down the side of the NMR tube, cooling to -78 °C before it reached the neopentyllithium. After addition was complete, the NMR tube assembly (stopcock closed) was transferred to the vacuum line, its contents frozen with liquid nitrogen, and the tube evauated and sealed. The NMR study was begun within 24 h of sample preparation. The sample was precooled to 200 K, and NMR spectra were obtained at the lower temperatures first.

Other samples prepared as described above were neopentyllithium with (a) 1,2-di(*N*-piperidino)ethane in THF-d_8, stable at 200 K for 1 month; (b) PMDTA in THF-d_8; (c) PMDTA in diethyl-d_{10} ether; (d) 1,4,7-trimetyl-1,4,7-triazacyclononane in THF-d_8. Unless otherwise stated all ligands were dried with Na/K immedately before distillation and preparation of samples.

Samples Prepared by Vacuum Transfer of Solvent. The following samples were prepared by bulb-to-bulb distillation of the solvent mixtures onto neopentyllithium in the NMR tubes, the latter cooled to 200 K: neopentyllithium in (a) methylcyclohexane-d_{14}, stable 6 months at room temperature; (b) THF-d_8, stable 1 week at 170 K; (c) diethyl-d_{10} ether, stable 1 month at 200 K; (d) diethyl-d_{10} ether-toluene-d_8, stable 1 month at 200 K; (e) 1,4,7-trimethyl-1,4,7-triazacyclononane in diethyl-d_{10} ether 2 months at 250 K. The rest of these preparations were the same as descried for neopentyllithium in THF-d_8-TMEDA.

Sample concentration were determined from the mode of preparation and integration of the low-temperature ^{13}C NMR spectra. Correction for the inevitable small degree of hydrolysis was accomplished by integration of the ^{13}C neopentane resonances observed in some spectra.

Acknowledgment. This research was generously supported by National Science Foundation Grant Nos. CHE 8304636 and 8817746 and in part by the Goodyear Tire and Rubber Co. The National Science Foundation also supported acquisition of two high-field NMR spectrometers used in this work. We thank Dr. Charles Cottrell, Campus Chemical Instrumentation Center, for helpful technical advice.

^1H NMR Study of the Role of Individual Heme Propionates in Modulating Structural and Dynamic Properties of the Heme Pocket in Myoglobin

Jón B. Hauksson, Gerd N. La Mar,* Ravindra K. Pandey, Irene N. Rezzano, and Kevin M. Smith

Contribution from the Department of Chemistry, University of California, Davis, California 95616. *Received January 8, 1990*

Abstract: The relative importance of the two heme propionate salt bridges to the protein matrix in determining the equilibrium orientational preference of the synthetic hemin, heptamethyl-monopropionate-porphine-iron(III), reconstituted into sperm whale and horse myoglobin metcyano complexes was determined using the nuclear Overhauser effect, NOE. The preferences for occupying the crystallographic 7-propionate position which makes a link to interior His FG3 in both proteins, versus that of the 6-propionate group interacting with the surface CD3 residue, were found to be ~1:2 for the sperm whale and 3:2 for the horse protein. Since the FG3 residue is conserved (His), and the CD3 residue differs in the two proteins (Arg for sperm whale, Lys for horse), we conclude that the 6-propionate-Lys CD3 link in horse Mb is less stable by ~0.64 kcal/mol than the 6-propionate-Arg CD3 salt bridge in sperm whale Mb. Since this salt bridge, in part, holds closed a likely distal ligation channel to the heme pocket, the lower stability of this link in the horse relative to the sperm whale protein provides a structural basis for interpreting earlier highly differential labile hydrogen dynamics for the two proteins (Lecomte, J. T. J.; La Mar, G. N. *Biochemistry* **1985**, *24*, 7388-7395). Reconstitution of horse Mb with protohemin IX derivatives having individual propionates selectivity replaced by methyls confirms that vinyl contacts are much more important than propionate contacts in determining the orientational preference of the heme in the pocket. Each of the monopropionate hemins revealed that the orientational isomer with a propionate in the crystallographic 6-position is in dynamic equilibrium (~10^3 s^{-1}) with another isomeric form which is deduced to be the heme orientation with the propionate in the crystallographic 8-position. The interconversion involves simply 90° rotational "hopping" of the heme about the iron-His bond, and this process is concluded to be significantly faster in the horse than sperm whale protein, again suggesting that the 6-propionate salt bridge is weaker in the former Mb.

Introduction

The binding of the heme prosthetic group within the pocket of myoglobin, Mb, is determined by a number of heme-protein interactions. These include the axial imidazole-iron bond, van der Waals interactions between hydrophobic amino acid side chains and the polarizable heme π system, salt bridges, and/or hydrogen bonds to the ubiquitous heme propionates, and possibly small steric influences resulting from protein constraints forcing vinyl side chains to be more in-plane than in model compounds.[1,2] It is possible to perturb significantly these heme-protein contacts and still retain strong heme binding as witnessed by the formation of strong holoprotein complexes in either the absence of a central metal to form the iron-His bond,[3] the esterification of both propionates,[4] or the wide range of chemical functionalization of

(1) Antonini, E.; Brunori, M. *Hemoglobin and Myoglobin in Their Reactions with Ligands*; North Holland Publishing Co.: Amsterdam, 1971; Chapter 13.

(2) (a) Takano, T. *J. Mol. Biol.* **1977**, *110*, 537-568. (b) Takano, T. *J. Mol. Biol.* **1977**, *110*, 569-584. (c) Phillips, S. E. V. *J. Mol. Biol.* **1980**, *142*, 531-534. (d) Kuriyan, J.; Wilz, S.; Karplus, M.; Petsko, G. A. *J. Mol. Biol.* **1986**, *192*, 133-154.

(3) Jameson, D. M.; Gratton, E.; Weber, G.; Alpert, B. *Biophys. J.* **1984**, *65*, 795-803.

(4) Tamura, M.; Asakura, T.; Yonetani, T. *Biochim. Biophys. Acta* **1973**, *295*, 467-479.

0002-7863/90/1512-6198$02.50/0

the heme periphery[5-7] of the hydrophobic portion (pyrroles A and B) of protohemin, **1**. The two propionates are oriented toward the hydrophilic portion of the heme cavity near the protein surface. The exact interactions are revealed in numerous X-ray crystal structures of sperm whale Mb,[2,6] where they form salt bridges, the 6-propionate to the surface Arg CD3, and the 7-propionate to the interior His FG3 stacked parallel to and over pyrrole C. However, one salt bridge (involving the 7-propionate and His FG3) may be more stable and important than the other, since the structure of sperm whale MbCO reveals[2d] only partial formation of the bridge to Arg CD3. Of intrinsic importance in understanding the structure and dynamic properties[8] of the heme pocket is a clear understanding of the relative importance of the various heme–protein interactions.

Previous work aimed at elucidating the role of individual propionates in stabilizing the heme pocket involved[9] reconstitution

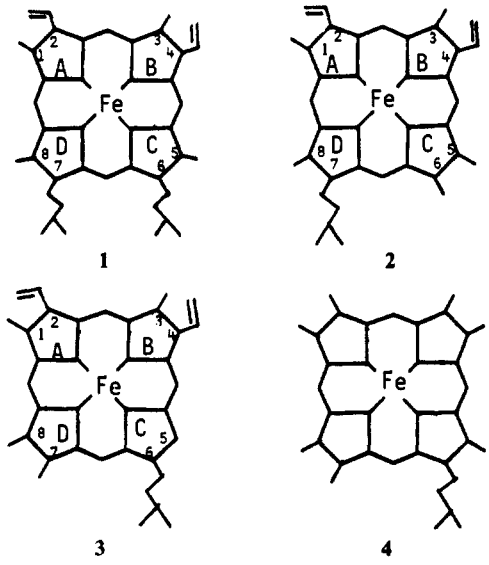

of sperm whale apo-Mb with protohemin IX derivatives where either the 6-propionate, **2**, or 7-propionate, **3**, is replaced by a methyl.[10] However, it was found,[9] that both of these modified hemes occupied the same orientation in the heme pocket with respect to the invariant vinyls, dictating that the asymmetric vinyl contacts with the protein are much more important than asymmetric propionate contacts in determining equilibrium heme orientational preferences.[9,11] Nevertheless, the identical position of the propionates in the heme pocket of the initially formed metastable species obtained immediately after reconstitution revealed[12] that the propionates dominate the structure of the initial encounter complex during reconstitution, while vinyls dominate the equilibrium orientation.

The ground-state structure of Mb[2,6,8] does not reveal an access pathway into the heme cavity for exogenous ligands, and hence the dynamic properties of the heme pocket, such as the "gating" of a trap door to the protein surface on the distal side, have been invoked.[13] One of the two propionates (6-position) in native Mb

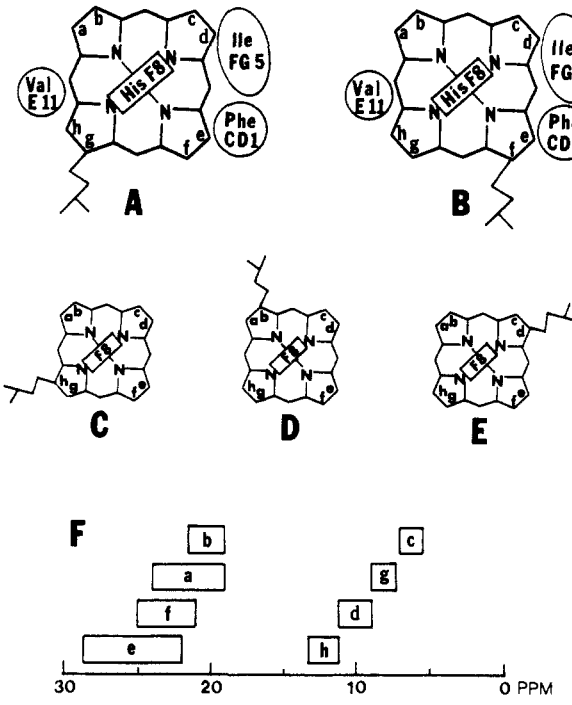

Figure 1. Schematic representation of hemin in the pocket of Mb relative to the invariant His F8 imidazole plane, and the Phe CD1, Ile FG5, and Val E11 side chains. The positions of potential heme substituents are identified by a labeling scheme referenced to the protein matrix identified by the letters $a \rightarrow h$ which are used as subscripts in identifying the resonances occupying these sites. The possible orientations of the sole propionate side chains of hemins **2**, **3**, and **4** considered in interpreting the NMR data are shown in A–E, and the molecular species possessing these heme orientations are referred to as isomers A–E, respectively. The native hemin, **1**, has its propionates at position *g* for the 7-propionate (as in A) and position *f* for the 6-propionate (as in B) for the heme orientations as found in the crystal structures.[2] A schematic representation of the range of heme methyl chemical shifts for the individual protein sites identified by *a–h* in A–E, is given in F, based on both previous and the current methyl assignments.[9,11,12,15,29]

is involved in a salt bridge with a residue (CD3) that holds closed a very likely ligation channel. The X-ray structure of phenyl-Mb,[14] which has the "trap door" held open by the large bound phenyl ligand, shows that this propionate salt bridge is broken. Hydrogen exchange studies with bulk solvent have similarly implicated[15] the breaking of the 6-propionate–CD3 residue salt bridge to allow access to the hydroxide ion. Moreover, the difference in exchange mechanism in structurally largely conserved sperm whale (Arg CD3) and horse (Lys CD3) was attributed[15] to differences in the stability of 6-propionate–Arg versus 6-propionate–Lys salt bridge, with the latter judged slightly weaker.

In this report we focus solely on the relative preferences of forming the FG3 versus CD3 salt bridges in sperm whale and horse myoglobins, and interpret these different preferences in terms of the relative stability of the CD3 bridge in sperm whale (Arg) and horse (Lys) Mb.[16] The two proteins are otherwise structurally identical in the heme cavity, as supported both by X-ray structures[2,17] and functional studies.[18] To this end, we have prepared[19] the synthetic hemin, heptamethyl–monopropionate–porphine–iron(III), possessing a single propionate group, **4**. The insertion,

(5) Reference 1, Chapter 4.
(6) Mibi, K.; Ii, Y.; Yukawa, M.; Owatari, A.; Hato, Y.; Harada, S.; Kai, Y.; Kasai, N.; Hata, Y.; Tanaka, N.; Kakuda, M.; Katsubi, Y.; Yoshida, Z.; Ogoshi, H. *J. Biochem.* **1986**, *100*, 269–276.
(7) Asakura, T.; Lau, P. W.; Sono, M.; Adachi, K.; Smith, J. J.; McCray, J. A. In *Hemoglobin and Myoglobin Oxygen Binding*; Ho, C., Ed.; Academic Press: New York, 1982; pp 177–184.
(8) Gurd, F. R. N.; Rothgeb, T. M. *Adv. Protein Chem.* **1979**, *33*, 73–105. (b) Karplus, M.; McCammon, A. D. *CRC Crit. Rev. Biochem.* **1981**, *9*, 293–349. (c) Debrunner, P. G.; Frauenfielder, H. *Annu. Rev. Phys. Chem.* **1982**, *33*, 283–299.
(9) La Mar, G. N.; Emerson, S. D.; Lecomte, J. T. J.; Pande, U.; Smith, K. M.; Craig, G. W.; Kehres, L. A. *J. Am. Chem. Soc.* **1986**, *108*, 5568–5573.
(10) Smith, K. M.; Craig, G. W. *J. Org. Chem.* **1983**, *48*, 4302.
(11) La Mar, G. N.; Toi, H.; Krishnamoorthi, R. *J. Am. Chem. Soc.* **1984**, *106*, 6395–6401.
(12) La Mar, G. N.; Pande, U.; Hauksson, J. B.; Pandey, R. K.; Smith, K. M. *J. Am. Chem. Soc.* **1989**, *111*, 485–491.
(13) Case, D. A.; Karplus, M. *J. Mol. Biol.* **1979**, *132*, 343–368.
(14) Ringe, D.; Petsko, G. A.; Kerr, D. E.; Ortiz de Montellano, P. R. *Biochemistry* **1984**, *23*, 2–4.
(15) Lecomte, J. T. J.; La Mar, G. N. *Biochemistry* **1985**, *24*, 7388–7395.
(16) Dayhoff, M. O. *Atlas of Protein Sequence and Structure*; National Biomedical Research Foundation: Washington, D.C., 1972; Vol. 5.
(17) Evans, S. V.; Brayer, G. D. *J. Biol. Chem.* **1987**, *263*, 4263–4268.
(18) Stetzkowski, F.; Cassoly, R.; Banerjee, R. *J. Biol. Chem.* **1979**, *254*, 11351–11356.
(19) Pandey, R. K.; Rezzano, I. N.; Smith, K. M. *J. Chem. Soc.* **1987**, 262–263.

at equilibrium, of **4** in the orientation as in A or B in Figure 1 will reflect the relative preferences for the two salt bridges without interference from the vinyl group preferences of the compounds **2** and **3**. The determination of the equilibrium-heme orientation and the characterization of the structural and dynamic properties will be carried out by ^{1}H NMR in the low-spin cyanide complex of the ferric protein, metMbCN, which has been shown to readily yield the needed information based on either 1D[9,20] or 2D[21] nuclear Overhauser effect,[22] NOE, measurements.

Experimental Section

Sample Preparation. Sperm whale and equine myoglobin, Mb, were purchased from Sigma and used without further purification. Apomyoglobin, apoMb, was prepared according to published procedures.[23] For metcyano Mb samples, solutions approximately 1.5 mM in apoMb in ^1H_2O were prepared by dissolving lyophilized apoMb in cold phosphate buffer (50 mM, pH 6.2–6.3). The precipitate, if any, was removed by centrifugation, and the final concentration of apoprotein was determined by optical absorption intensity (ϵ = 15 900 M^{-1} cm^{-1} at 280 nm).

The hemins were prepared as reported previously,[10,19] and solutions of hemin were prepared by dissolution in a mixture of pyridine and 0.2 M NaOH in the presence of 5–6-fold excess potassium cyanide. The organic cosolvent and cyanide ligand are necessary to dissolve these modified, relatively insoluble, hemins.[9,12] Each reconstituted protein was prepared by dropwise addition of 1 molar equiv of the hemin solution to the chilled apoMb solution. For each sample the incorporation of hemin into apoMb was monitored optically according to published procedures.[24] Hemin was added in small and equal aliquots to a sample cell containing apoMb in 50 mM phosphate buffer at pH 7 and a reference cell containing only the buffer. The increase in optical intensity of the Soret band was monitored. The abrupt change in the slope of the titration curve at 1:1 molar ratio establishes the quantitative incorporation of stoichiometric amounts of each hemin into apomyoglobin. The organic solvent was immediately removed by passing the reconstituted holoprotein sample down a Sephadex G-25 column.[25] The protein was subsequently ultrafiltered in an Amicon ultrafiltration cell to raise the concentration, and the solvent was exchanged several times with ^2H_2O, 0.2 M in NaCl and 0.020 M in KCN, pH = 8.5. The sample pH was measured with a Beckman 3550 pH meter equipped with an Ingold micro-combination electrode; pH values were not corrected for the isotope effect.

Monopropionate–heptamethyl–hemin, **4**, reconstituted sperm whale metMbCN, was reduced to the deoxy state with sodium dithionite, rigorously excluding air from the sample by keeping all solutions under an atmosphere of nitrogen. Carbon myoglobin was prepared from the deoxy protein by bubbling carbon monoxide gas through the sample for 15 min. Dithionite and unwanted ions were subsequently removed by passing the sample through a Sephadex G-25 column. Finally, the purified carbon monoxy myoglobin sample was oxidized to the met-aquo state with potassium ferricyanide.

^{1}H NMR Measurements. ^{1}H NMR spectra were recorded on Nicolet/GE NT-500 and NT-360 FT NMR spectrometers using quadrature phase detection at 500 and 360 MHz, respectively. For the metcyano myoglobin, metMbCN, samples, spectra were obtained at 500 MHz in double precision by collecting 16 384 data points over a 14-kHz bandwidth at a pulse repetition rate of 1 s^{-1}. For the deoxy and met-aquo myoglobin samples, spectra were recorded at 360 MHz by collecting 8192 data points over a 55-kHz bandwidth at a pulse repetition rate of 8 s^{-1} and 8192 data points over a 45-kHz bandwidth at a pulse repetition rate of 10 s^{-1}, respectively. In all cases the residual water signal was suppressed with a low-power decoupler pulse.

The NMR spectra of the metMbCN complexes of **2**, **3**, and **4** were run at 25 °C as soon as practical after preparation (~1–4 h) and again after 10 to 14 days and 3 months to ensure that equilibrium had been reached.[9,11,12] The pH profile of the chemical shifts and line widths of sperm whale metMbCN reconstituted with **4** was recorded at 25 °C in ^2H_2O in the range 6 to 10 by titrating from the acidic side with 0.2 M NaO^2H in ^2H_2O. The nuclear Overhauser effect, NOE, difference spectra were recorded by applying a presaturation pulse of 200-ms duration with the decoupler on resonance, and subtracting the trace from the corresponding reference spectra recorded under identical conditions but with the decoupler off resonance. On- and off-resonance frequencies were alternated every 100 scans. Typical spectra consisted of at least 2600 transients with a repetition rate of 1 s^{-1}. The steady-state NOE is defined as the fractional change in intensity of peak i while peak j is being saturated, i.e.

$$\eta_{j\rightarrow i} = \frac{I_{zi} - J_{zi}^0}{I_{zi}^0} = \frac{\sigma_{ij}}{\rho_i} \quad (1)$$

where σ_{ij} is the cross relaxation rate that is proportional to r_{ij}^{-6}, and ρ_i is the intrinsic spin–lattice relaxation rate.[22] The nonselective spin–lattice relaxation times for the sperm whale metMbCN complex reconstituted with **4** were determined by the conventional inversion–recovery technique, and the T_1 were obtained from the initial slope of the semilogarithmic plots. Line widths, in Hz, were determined by simulation using the NTCAP simulation program of the Nicolet 1280 software. Chemical shifts are given in parts per million (ppm) from internal 2,2-dimethyl-2-silapentane-5-sulfonate (DSS) via the residual solvent resonance.

Results

Resonance Assignment Strategy. In order to determine the orientations within the pocket of the hemins **2**–**4**, the physical location of the sole propionate in the protein matrix must be established in each case; for practical reasons, this is more readily achieved by identifying the environments of all heme methyl and/or vinyl groups. The location of a substituent, R_i, on a heme is more conveniently referred to by position in the protein matrix rather than by its relative position on the heme. The subscript i is identified in the heme pocket sites in Figure 1. The determination of the heme orientation relates the heme-based and protein-based labeling schemes. We therefore adopt the "site-labels" for substituent R_i by the subscripts $a \rightarrow h$ that identify the locations of the substituents as shown in Figure 1; the positions $a \rightarrow h$ are occupied by substituents 1 → 8 for protohemin, **1**, in the X-ray-determined orientation of Mb.[2,17] Two strategies are pursued. On the one hand, NOE connectivities between individual heme substituents and specific amino acid side chains determine the spatial disposition of a given heme substituted in an essentially unperturbed heme pocket.[9,20] The residues readily identified by large and unique hyperfine shifts and intra-residue NOE patterns are the low-field shifted Phe CD1[26] (with contacts solely to R_e), and the upfield shifted Ile FG5[27] (δ-CH_3 contact solely to R_d and R_c, γ-CH_3 contact to both R_e and R_d), and Val E11[9,21] ($C_\alpha H$ contact to R_h); another useful diagnostic contact is the His FG3 ring $C_\delta H$ at ~7 ppm[7,21] (solely to R_f). The relative positions of two heme methyls are identified by ~−4% NOE for methyls adjacent on the same pyrrole, and ~−1% NOEs between two methyls adjacent to the same meso-H, as discussed in detail previously.[9]

An auxiliary approach to assignments makes use of the characteristic contact shift pattern exhibited by heme methyls that reflect solely the position of a methyl on a heme relative to the His F8 imidazole plane.[28,29] This pattern hence reflects the protein-based rhombic perturbation and represents a second method for characterizing the location of a methyl in the heme pocket by its hyperfine shift.[9] The unique and limited ranges of methyl hyperfine shift as a function of position in our protein-based labeling scheme, a–h, as determined on a variety of derivatives via isotope labeling and NOEs,[9,28,29] are reproduced in F of Figure 1. Thus the lowest field methyl peak occurs for position a, and shifts for positions a, b, e, f are always much larger than for position c, d, g, h, with h, d generally resolved on the low-field side of the intense diamagnetic envelope, and methyls g, c under this envelope. The observation of this expected methyl contact shift pattern (F of Figure 1), as well as invariant dipolar shifted

(20) Lecomte, J. T. J.; Johnson, R. D.; La Mar, G. N. *Biochim. Biophys. Acta* **1985**, *829*, 268–274.
(21) Emerson, S. D.; La Mar, G. N. *Biochemistry* **1990**, *29*, 1545–1555.
(22) Neuhaus, D.; Williamson, M. *The Nuclear Overhauser Effect*; VCH Publishers: New York, 1989; Chapter 2.
(23) Teale, F. W. J. *Biochim. Biophys. Acta* **1959**, *35*, 543.
(24) Asakura, T.; Yonetani, T. *J. Biol. Chem.* **1969**, *244*, 4573–4579.
(25) Johnson, P. D.; Figueroa, N.; Redfield, A. G. *Proc. Natl. Acad. Sci. U.S.A.* **1979**, *76*, 3130–3134.
(26) Emerson, S. D.; Lecomte, J. T. J.; La Mar, G. N. *J. Am. Chem. Soc.* **1988**, *110*, 4176–4182.
(27) Ramaprasad, S.; Johnson, R. D.; La Mar, G. N. *J. Am. Chem. Soc.* **1984**, *106*, 5330–5335.
(28) Shulman, R. G.; Glarum, S. H.; Karplus, M. *J. Mol. Biol.* **1971**, *57*, 93–115.
(29) La Mar, G. N. In *Biological Applications of Magnetic Resonance*; Shulman, R. G., Ed.; Academic Press: New York, 1979; pp 305–340.

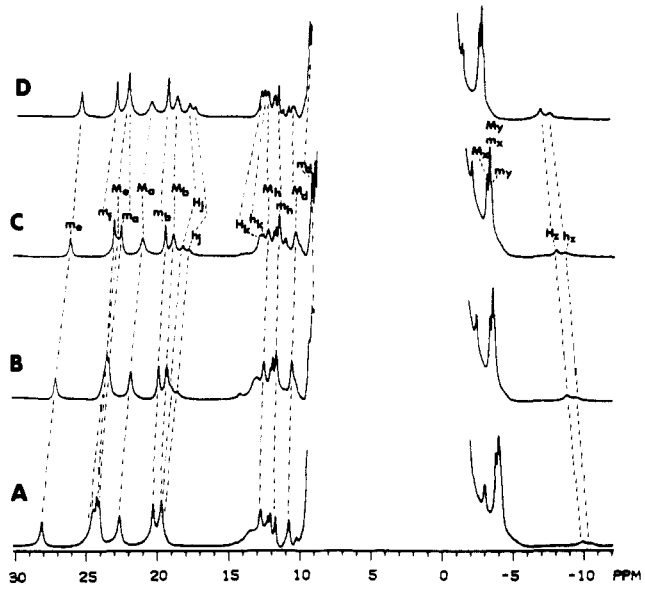

Figure 2. Resolved portions of the 500-MHz ^1H NMR spectra of equilibrated sperm whale metMbCN reconstituted with hemin **4**, in ^2H_2O at pH 8.6, as a function of temperature: (A) 5°, (B) 15°, (C) 25°, and (D) 35 °C. The two sets of peaks are identified by either upper or lower case letters. M_i, m_i (methyls) and H_i, h_i (nonmethyls), with the sets m_i, h_i and M_i, H_i originating from the isomers as in A and B, respectively, of Figure 1, and are most readily differentiated by the different methyl line widths. The subscripts identify the position of substituents on the heme (*a–h*) as located in the protein matrix (see Figure 1), or previously identified[26,27] amino acid signals Phe CD1 (*j*, *k*), His FG3 $C_\delta H$ (*m*), Val E11 $C_\alpha H$ (*v*), and Ile FG5 $C_\gamma H'$, $C_\gamma H_3$, $C_\delta H_3$, $C_\gamma H$ (*w*, *x*, *y*, *z*).

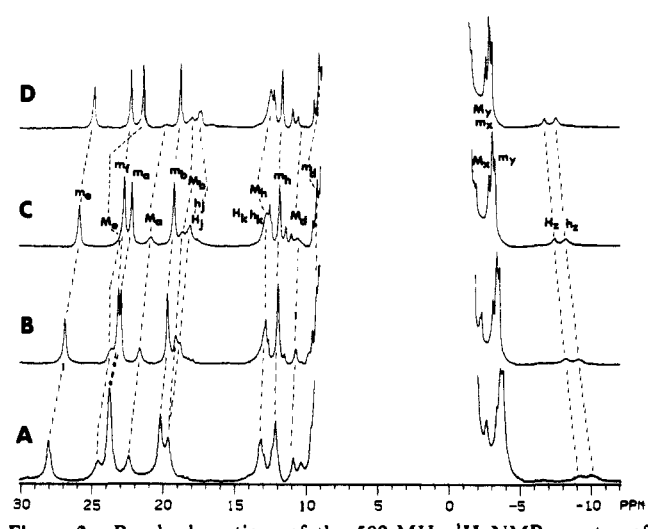

Figure 3. Resolved portions of the 500-MHz ^1H NMR spectra of equilibrated horse metMbCN reconstituted with **4**, in ^2H_2O at pH 8.6, as a function of temperature: (A) 5°, (B) 15°, (C) 25°, and (D) 35 °C. Peaks are designated as in Figure 2.

Phe CD1, Ile FG5, and Val E11 resonances, provides direct evidence that the protein folding and heme electronic/magnetic structures are conserved upon perturbing the heme periphery.[30]

Orientation(s) for Hemin 4. The resolved portions of the 500-MHz ^1H NMR spectra of equilibrated sperm whale and horse metMbCN complexes reconstituted with heptamethyl–monopropionate–porphine–iron(III), **4**, as a function of temperature are illustrated in Figures 2 and 3, respectively. Several of these resonances overlap at any one temperature, but following the traces as a function of temperature allows us to identify the position of all resonances. Both proteins exhibit a pair of resolved (apparent) single proton resonances, H_z, h_z in the −7 to −10 ppm region where only Ile FG5 $C_\gamma H$ resonates,[9,21,27] and nine signals with intensities

(30) Emerson, S. D.; La Mar, G. N. *Biochemistry* **1990**, *29*, 1556–1566.

Table I. NMR Spectral Parameters for the Two Heme Orientations of Heptamethyl–Monopropionate–Porphine–Iron(III) Reconstituted into Sperm Whale and Horse metMbCN[a]

		isomer A m_i, h_i shifts[a,b]		isomer B M_i, H_i shifts[a,c]	
subscript i	assignment	sperm whale	horse	sperm whale	horse
a	heme[d]	20.9 (110)[e]	20.7	22.4	22.0
b	heme	18.7	18.6	19.3 (110)[c]	19.1
c	heme	5.7	*g*	5.6	*g*
d	heme	10.2 (180)	10.5	9.0	9.0
e	heme	22.6 (135)	22.5	25.9 (130)	25.8
f	heme	8.8[f]	*g*	22.9 (155)	22.6
g	heme	7.5	*g*	2.0[f]	*g*
h	heme	12.0 (200)	12.3	11.3 (180)	11.7
j	PheCD1 $C_\zeta H$	17.7 (17)	18.1	17.2 (19)	18.0
k	PheCD1 $C_\eta H$	12.6 (70)	12.4	12.4 (80)	12.2
w	Ile FG5 $C_\gamma H'$	−1.2		−1.4	
x	Ile FG5 $C_\gamma H_3$	−3.2	−2.9	−3.4	−3.2
y	Ile FG5 $C_\delta H_3$	−3.4	−3.2	−3.6	−3.3
z	Ile FG5 $C_\gamma H$	−8.1 (75)	−7.5	−8.7 (76)	−8.3

[a] All data at 25 °C in ^2H_2O solution at pH 8.6; chemical shifts in ppm from DSS. [b] Hemin orientation as shown in A of Figure 1. [c] Heme orientation as shown in B of Figure 1. [d] Heme methyl unless noted otherwise. [e] Nonselective T_1 values, in ms, for sufficiently resolved resonances, are given in parentheses. [f] Heme propionate H_α.

of three times of H_z, h_z, indicative of methyls in a region where a single orientation as in A or B of Figure 1 should produce only four or five methyl signals. Hence both of the proteins reconstituted with hemin **4** must possess at least two different heme orientations at equilibrium. An inspection of the traces reveals a characteristic difference in the low-field line-width patterns that allow differentiation of the two subsets of signals. The apparent methyl peaks labeled m_i exhibit narrow lines at 25 °C (50–70 Hz), as found in the native proteins.[9,26] The second set of apparent heme methyl peaks, labeled M_i, are considerably broader (120–200 Hz) and become broader as the temperature rises, particularly for the horse metMbCN complex (Figure 3). Integration of the optimally resolved methyl peaks m_e and M_a (or single proton peaks h_z and H_z) for the presumed two isomeric forms at 25 °C yields a ratio of m_i:M_i ~ 1:2 for sperm whale (C of Figure 2) and ~3:2 for horse metMbCN (C in Figure 3). The large line widths, particularly at higher temperatures, do not allow sufficiently accurate integration to unambiguously establish changes in the ratio of isomers with temperature.

Generation of the sperm whale deoxy protein by reduction of hemin **4** reconstituted metMbCN by dithionite, conversion to the carbonyl complex by bubbling CO through the deoxy Mb solution, and conversion of the met-aquo complex upon removal of CN^- from the MbCO complex prior to oxidation by ferricyanide yielded NMR spectra characteristic of comparable amounts of two species[9,29] [i.e., two His F8 NH peaks at ~76 ppm in deoxy Mb, two Val E11 γ_2-CH_3 at ~−2.5 ppm[9] in MbCO, and ~14 methyl peaks in the region 50–90 ppm in metMbH_2O (not shown)]. Moreover, the ratio of peaks did not change detectably over 12–24 h and, upon re-formation of the metMbCN complex, yielded an ^1H NMR spectrum essentially identical with that in C of Figure 2. Hence the relative stabilities of the two isomers do not appear to be significantly affected by the oxidation/ligation state of the heme.

Variation of the solution pH in the range 5.8 to 9.5 for the sperm whale metMbCN complex of hemin **4** revealed only small shift changes near pH 6, as found for native metMbCN[31] (not shown). The line widths of the hyperfine shifted resonances, in particular, the anomalously broadened heme methyl peaks, M_i, are unaffected by pH. A determination of the nonselective spin–lattice relaxation times yields the values listed in Table I. The shortest T_1s are found for the pairs of signals h_j, H_j (~20 ms), h_k, H_k (~80 ms), and h_z, H_z (~60 ms). The remainder of the resolved methyls

(31) Krishnamoorthi, R.; La Mar, G. N. *Eur. J. Biochem.* **1984**, *138*, 135–140.

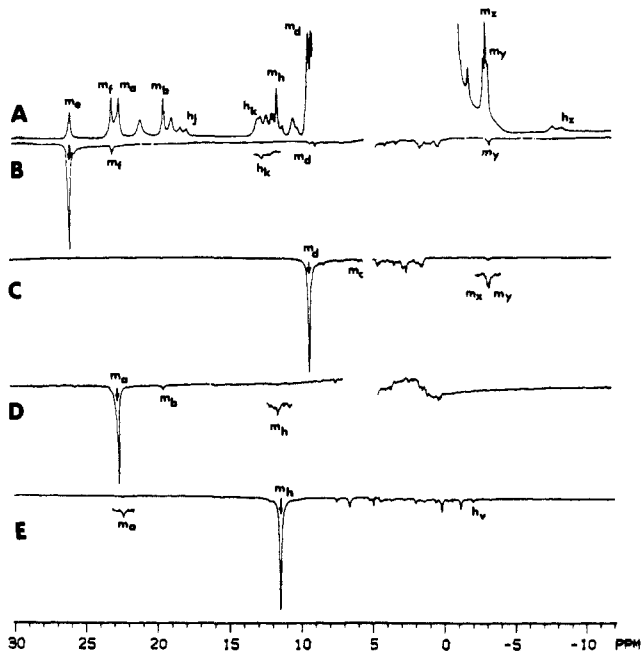

Figure 4. Identification of peaks m_i, h_i for isomer A of sperm whale metMbCN reconstituted with hemin **4** in ^2H_2O at 35 °C, pH 8.6. (A) reference ^1H NMR spectrum; peaks are labeled for one of the two isomers m_i, h_i, as defined in the caption to Figure 2. (B–E) NOE difference spectra upon saturating the resonance indicated by a vertical arrow. (B) Saturate m_e; note ~ −5 and ~ −1% NOE to heme methyl signals, m_f and m_d, respectively, as well as NOEs to amino acid signal h_k (Phe CD1 $C_\epsilon Hs$) and m_y (Ile FG5 $C_\gamma H_3$). (C) Saturate m_d; note NOE to m_x, m_y (Ile FG5, $C_\gamma H_3$, $C_\delta H_3$). (D) Saturate m_a; note ~ −4 and ~ −1% NOEs to heme methyl peak m_b and m_h, respectively. (E) Saturate m_h; note reciprocal NOE to m_a, as well as characteristic[9,24] upfield NOEs, including Val E11 $C_\alpha H$, (h_v).

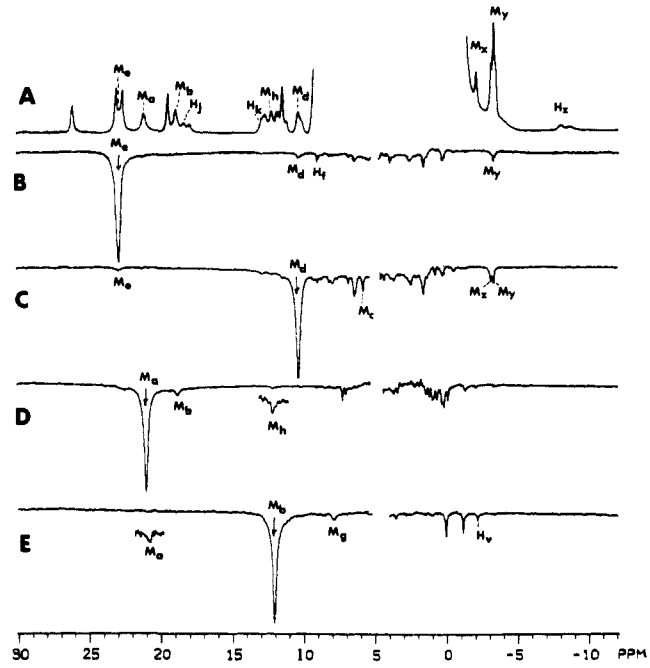

Figure 5. Identification of peaks M_i, H_i, for isomer B of sperm whale metMbCN reconstituted with hemin **4**, in ^2H_2O, at 35 °C, pH 8.6. (A) Reference ^1H NMR spectrum; peaks are labeled for one of the isomer M_i, H_i, as defined in Figure 2. (B–E). NOE difference traces upon saturating the resonance indicated by a vertical arrow. (B) Saturate M_e; note small NOE to heme methyl peak M_d, Ile FG5 $C_\delta H_3$ peak M_y, and apparent heme propionate H_α peak H_f (the trace has been computer corrected for off-resonance saturation of the flanking narrower m_f and m_a peaks). (C) Saturations of M_d; note NOEs to M_c and M_e (also seen from M_y) as well as to Ile FG5 methyls M_x, M_y. (D) Saturate M_a; note ~−5 and ~−1% NOEs to heme methyls M_b and M_h, respectively. (E) Saturate M_h; note reciprocal NOE to M_a, as well as upfield NOEs including Val E11 $C_\alpha H$ (H_v) that characterize[9,21] position h.

yielded T_1s in the range 110–150 ms, as found for native metMbCN.[26,27,32] The rapidly relaxing signals with subscripts *j*, *k*, *z* with similar shifts in native metMbCN originated from Phe CD1 and Ile FG5 protons close to the heme.[26,27] Proof that a set of peaks m_i and M_i arises from separate molecular entities, as well as the identification of amino acid peaks with each species and the assignment of the methyls, result from the detailed NOE studies described below. Such assignments are pursued solely for the sperm whale metMbCN complex of hemin **4**.

(i) **Minor Isomer Heme Orientation.** The 35 °C reference trace of sperm whale metMbCN reconstituted with hemin **4** is shown in Figure 4A, with peaks labeled m_i (methyls) and h_i (nonmethyls) for this isomer. Saturation of h_z yields an NOE pattern diagnostic[9,27] of Ile FG5 $C_\gamma H$, leading to the assignments $m_x = C_\gamma H_3$, $m_y = C_\delta H_3$, and $h_w = C_\gamma H'$ (not shown). Similarly, saturation of the fast relaxing (T_1 ~ 20 ms) single proton peak, h_j, yields an NOE to a two-proton peak, h_k, with T_1 ~ 80 ms (not shown); the shifts, relaxation, and NOE patterns are diagnostic[9,26] for the $C_\zeta H$ and averaged $C_\epsilon Hs$, respectively, for a rapidly reorienting ring of Phe CD1. Saturation of m_e yields an NOE to Ile FG5 $C_\delta H_3$ (m_y) and Phe CD1 $C_\epsilon Hs$ (h_k) (Figure 4B), which is diagnostic of a methyl at position *e* in A, B of Figure 1. The ~ −5% NOE to peak m_f and ~ −1% NOE to peak m_d identify heme methyls at positions *f* and *d*, respectively. The assignment of m_f is confirmed by the characteristic NOE to a sharp peak at 7 ppm (not shown), previously shown to arise from His FG3.[9,21] The assignment of m_d is confirmed by the comparable NOEs to both Ile FG5 methyls, m_x, m_y (Figure 4C), and the weak NOE to peak m_c at 5.7 ppm, together with a larger NOE from Ile FG5 $C_\gamma H_3$ to m_c (not shown) identify m_c as the methyl at position *c* in Figure 1. Irradiation of m_a yields a ~ −5% NOE to m_b and a ~ −1% NOE to m_h (Figure 4D), and saturation of m_h yields NOEs characteristic of a methyl at position *h* (Figure 4E); this uniquely assigns m_a, m_b, and m_h to methyls at positions *a*, *b*, and *h* in Figure 1. Hence methyls unequivocally occupy all positions in the protein matrix except position *g*, which must be occupied by the sole propionate, and we can conclude that the isomer with the "normal" line widths with peaks m_i, h_i arises from the heme orientation as shown in A of Figure 1. The similar shifts and line widths of peaks m_i for the sperm whale and horse metMbCN complexes of hemin **4**, as also found for native protein,[15] dictate the same assignments in the two proteins. The assignments and the chemical shifts at 25° are summarized in Table I.

(ii) **Major Isomer Heme Orientation.** The reference trace at 35 °C labeling the peaks M_i, H_i from this isomer is reproduced in Figure 5A. Saturation of the rapidly relaxing single-proton upfield peak, H_z, and downfield peak, H_j, resulted in NOE patterns (not shown) very similar to those observed for the analogous minor component peaks h_z and h_j, and yield the assignments for Ile FG5 peaks, $C_\delta H_3$ (M_y), $C_\gamma H_3$ (M_x), $C_\gamma H'$ (H_w), and Phe CD1 peaks H_j ($C_\zeta H$) and H_k ($C_\epsilon Hs$), as shown in detail previously for similar protein complexes.[26,27] Saturation of M_e yields a small NOE to M_d and Ile FG5 $C_\delta H_3$ (M_y), identifying M_e and M_d as the methyls of position *e* and *d* of Figure 1; the absence of an NOE from M_e to another strongly shifted methyl in the 15–25-ppm region argues against a methyl at position *f* of Figure 1, and leads to the anticipated conclusion that this isomer must have the propionate at position *f*. Saturation of M_d yields the expected comparable NOEs to the two Ile FG5 methyls (Figure 5C); a weaker NOE to 5.6 ppm, which is also observed from Ile FG5 $C_\gamma H_3$ (not shown), identifies M_c as the methyl at position *c*. Saturation of M_a (Figure 5D) and M_b (not shown) yields the reciprocal NOEs indicative of adjacent methyls; the weaker NOE from M_a to M_h, as well as the diagnostic NOE from M_h to the three upfield peaks *g* (Figure 5E), uniquely identifies M_a, M_b, and M_h as the methyls at positions *a*, *b*, and *h* in Figure 1. Hence the seven methyls occupy all positions except *f*, where the lone propionate is situated with structure as in B of Figure 1. Again, the nearly identical

(32) Cutnell, J. D.; La Mar, G. N.; Kong, S. B. *J. Am. Chem. Soc.* **1981**, *103*, 3567–3572.

Table II. Chemical Shifts for Assigned Resonances for the Two Heme Orientations of 6-Methyl-6-despropionate hemin, **2**, and 7-Methyl-7-despropionate hemin, **3**, Reconstituted into Sperm Whale and Horse metMbCN[a]

		isomer A m_i, h_i shifts		isomer B M_i, H_i shifts		isomer A m_i, h_i shifts		isomer B M_i, H_i shifts	
i	assignment	sperm whale[b]	horse	sperm whale[b]	horse	sperm whale[b]	horse	sperm whale[b]	horse
a	heme[c]	19.0 (1)[c]	18.9 (1)	*e*	*e*	17.8 (1)	17.8 (1)	*e*	*e*
b	heme[c]	16.8 (2)[d]	18.2 (2)[d]	17.3 (3)	17.3 (3)	17.3 (2)[d]	17.5* (2)[c]	18.1 (3)	18.0 (3)
e	heme[c]	28.1 (5)	28.0 (5)	24.7 (8)	24.8 (8)	24.9 (5)	24.7 (5)	28.6 (8)	28.4 (8)
f	heme[c]	22.6 (6)	22.5 (6)	*f*	*f*	*f*	*e*	21.4 (7)	21.4 (7)
h	heme[c]	12.1 (8)	12.5 (8)	13.2 (5)	13.6 (5)	13.1 (8)	13.4 (8)	12.1 (5)	12.5 (5)
j	Phe CD1 $C_\zeta H$	15.5	17.1	16.1	16.3	17.3	17.3	*g*	*g*
x	Ile FG5 $C_\gamma H_3$	−3.0	−3.2	*g*	−3.2	−3.4	−3.0	*g*	*g*
y	Ile FG5 $C_\delta H_3$	−3.7	−3.5	*g*	−3.3	−3.8	−3.4	*g*	*g*
z	Ile FG5 $C_\gamma H$	−9.0	−8.9	−7.7	−8.6	−8.6	−7.9	*g*	*g*

[a] Chemical shifts at 25 °C in ppm from DSS for ^2H_2O solution at pH 8.6. [b] Data taken from ref 12. [c] Shifts given for heme methyls unless indicated otherwise; the identification of the methyl or vinyl H_α on the conventional heme numbering system (i.e., **2**, **3**) is given in parentheses after the chemical shift. [d] Heme 2-vinyl H_α resonance. [e] Not resolved. [f] Propionate H_α peak for this position not identified. [g] Too weak to detect clearly.

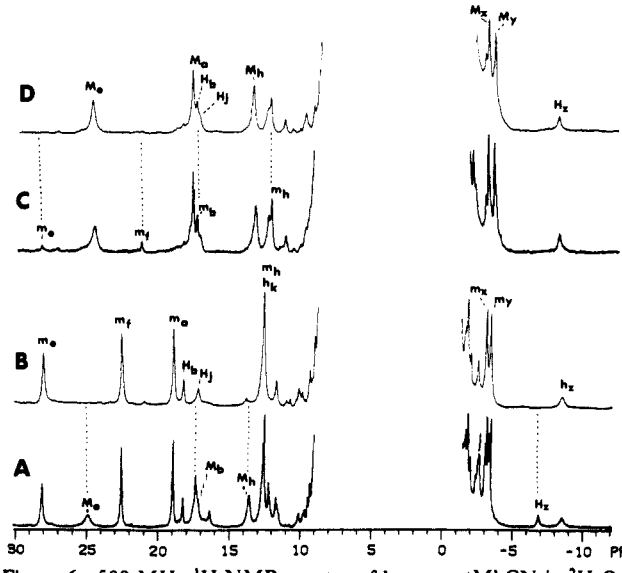

Figure 6. 500-MHz ^1H NMR spectra of horse metMbCN in ^2H_2O at 25 °C, pH 7.5, reconstituted with hemin **2** shortly after reconstitution (A) and after reaching equilibrium (B), and with hemin **3** shortly after reconstitution (C) and upon reaching equilibrium (D). The peaks are labeled m_i, h_i and M_i, H_i for the orientations as in A and B, respectively, in Figure 1. Peak assignments are completely by analogy to the previously reported[9,12] spectra for the same complexes of sperm whale metMbCN. Note that the set of peaks M_i are considerably broader than the set m_i for both hemins.

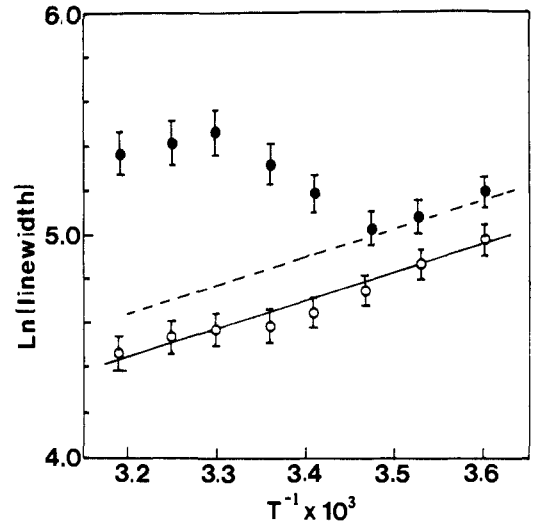

Figure 7. Plot of ln (line width) versus reciprocal temperature for heme methyl peaks for each of isomers A (m_e, O) and isomer B (M_a, ●) of sperm whale metMbCN reconstituted with heptamethyl-monopropionate porphine-iron(III), **4**, in ^2H_2O at pH 8.6.

chemical shifts allow these assignments to be extended to the horse protein. The assignments and chemical shifts are included in Table I.

Despropionate Hemin Complexes of Horse Mb. The ^1H NMR spectra of equilibrated sperm whale metMbCN reconstituted with 6-methyl-6-despropionate-hemin (**2**) and 7-methyl-7-despropionate-hemin (**3**) have been reported and assigned,[9,12] and the orientations shown to have the vinyls positioned as for native proteins, i.e., vinyls at positions *b* and *d* of Figure 1, so that the propionates for hemins **2** nd **3** occupied the positions as in A and B, respectively, of Figure 1. In Figure 6 we present the ^1H NMR spectra of horse metMbCN reconstituted with hemins **2** and **3**, some time shortly after reconstitution (traces A and B, respectively) and at equilibrium (traces B and D, respectively). As found previously for sperm whale Mb,[9,12] initially two orientations are present, characterized by sets of peaks m_i, h_i and M_i, H_i, with one set disappearing with time to yield an essentially (≥95%) homogeneous protein. For hemin **2**, the isomer with peaks m_i, and for **3**, the isomer with set M_i, exist as the dominant species at equilibrium. The chemical shifts for complexes of both hemins **2** and **3** are essentially the same as those for the previously published sperm whale complexes,[9,12] both for the intermediate as well as for the equilibrium complex (see Figures 3 and 4 of ref 12). Hence we conclude that the equilibrium orientations for hemins **2** and **3** for the propionates are as in A and B, respectively, of Figure 1. The resonances are assigned by analogy to the sperm whale metMbCN complexes[2,9] and the chemical shifts are listed in Table II, along with the previously reported data for hemins **2** and **3** in sperm whale metMbCN.

While the chemical shifts for hemins **2** and **3** are essentially the same in horse and sperm whale metMbCN for each of the two orientations (Table II), we note important differences in line-width patterns. For sperm whale metMbCN reconstituted with hemins **2** and **3**, the methyls for both heme orientations were found[9,12] narrow (50–70 Hz) and similar to those of native metMbCN. In the present complexes with horse metMbCN, we note that the intermediate species (peaks m_i) for hemin **3** exhibits narrow or "normal" methyl lines, while the final product (peaks M_i) exhibits anomalously broad lines (see C and D of Figure 6). Conversely, for hemin **2**, the intermediate with orientation as in B of Figure 1 yields anomalously broad methyl lines, M_i, while the final produced with orientation as in A of Figure 1 yields the "normal" narrow methyl lines, m_i (A and B in Figure 6). We also note that the anomalous broadening of methyl peaks M_i relative to the "normal" peaks m_i for hemin **4** reconstituted into metMbCN is much more severe for the horse (Figure 2) than the sperm whale (Figure 3) protein. Plots of the ln (line width) versus reciprocal temperature for the optimally resolved methyl peaks m_e and M_a for sperm whale metMbCN reconstituted with hemin **4** are illustrated in Figure 7. While peak m_e for isomer A exhibits the normal straight line (solid line) as found for the native protein,[26] with line width decreasing as the temperature is raised, the peak M_a approaches "normal" behavior (dotted line) only at very low temperature, with the peak line width increasing sharply with increasing temperature above 15 °C. This increase in line width with temperature is more dramatic for the horse than sperm whale

proteins. For the former complex, the line widths actually appear to reach a maximum at 30° and then decrease slightly. From the fact that only the M_i peaks exhibit this anomalous broadening of the various metMbCN complexes of hemins **2**, **3**, and **4**, we deduce that the line broadening is associated exclusively with the propionate orientation as in B of Figure 1, that the degree of line broadening for the same propionate orientation is much more severe in the absence of vinyl groups, and that this degree of line broadening is larger for the horse than the sperm whale metMbCN complex for any given hemin.

Discussion

Molecular/Electronic Structure. The very similar hyperfine shifts for the assigned amino acid resonances, in particular those for Phe CD1 and Ile FG5, argue for essentially invariant magnetic properties of the iron, as well as conserved stereochemistry for the heme pocket residues.[9,12,30] The largely unperturbed electronic properties of the heme are witnessed by the remarkable adherence of the heme methyl contact shift pattern (i.e., see F of Figure 1) to that determined for the native protein and that reconstituted with other hemes bearing normal pairs of propionate side chains.[9,12,21,29] Moreover, although the heme methyl signals for the alternate orientations exhibit markedly different line widths, the T_1 values for similarly contact shifted peaks, as well as those for the noncoordinated amino acid signals, are within experimental error of each other, such that the electron spin–lattice relaxation time is also the same. Hence the heme seats in the pocket in a well-defined orientation with respect to the proximal His F8 imidazole plane, and that orientation is unaffected whether either of the propionate salt bridges is abolished.

Relative Stabilities of the Propionate Salt Bridges. Compared to the dominant role played by the asymmetric vinyl groups in controlling the heme orientational preference[11] for native hemin, **1** ($K \sim 20$ or $\Delta G \sim 1.8$ kcal), the asymmetric placement of the propionates imparts only minor preference ($K_{eq}[A \rightarrow B] \sim 2$) in sperm whale Mb, and less ($K_{eq}[A \rightarrow B] \sim 0.7$) in horse Mb. This dictates that the relative contributions of the salt bridges at position 6 and 7 toward the binding free energy of native hemin are not substantially different. In sperm whale Mb, the 6-propionate salt bridge appears *more stable* than the 7-propionate link by ~400 cal. In the horse Mb, the 6-propionate link to the protein appears ~240 cal *less stable* than the 7-propionate salt bridge. The crystal structures of both sperm whale and horse Mb have been determined.[2,17] One salt bridge involves the 7-propionate (in position *g* in Figure 1) to the identically situated His FG3 on the highly conserved proximal side of the heme of both Mb's. The 6-propionate (in position *f* in Figure 1) forms a salt bridge to residue CD3, which is Arg in the sperm whale and Lys in the horse protein.[16] Since the 7-propionate link is identical, the small difference in the two salt bridges between sperm whale and horse Mb indicate that the salt bridge to position CD3 is more stable for Arg than Lys by ~0.64 kcal.

These conclusions support previous analysis of the labile proton exchange of the distal His E7 with bulk water for the two proteins.[15] Such exchange is facilitated by the opening of the ligation channel to the heme pocket for hydroxyl ion access,[33] and this opening requires the rupture of the propionate–CD3 but not the propionate–FG3 residue salt bridges.[14,15] Since the base-catalyzed exchange of distal His E7 $N_\epsilon H$ was found considerably faster in the horse than sperm whale metMbCN complex, the open pocket was judged more stable and hence implies a less stable propionate to CD3 residue link in the former protein.[15] However, since the exchange rate differential indicated a ~2.1-kcal/mol difference in the relative stabilities of the open versus closed ligation channel,[15] the presently characterized ~0.6-kcal/mol difference does not represent the dominant contribution. This larger contribution must therefore originate from the Arg versus Lys CD3 salt bridge with Asp E3, which also must be broken upon opening the channel.[14]

A more detailed and quantitative thermodynamic analysis of the two propionate links for hemin **4** is complicated by observations which suggest that, while the two major propionate orientations for a single propionate-containing heme are precisely the ones occupied by the two propionates in native hemin (i.e., A and B in Figure 1), at least one additional minor component must exist which possesses a propionate group at a position different from that shown in either A or B of Figure 1.

Heme Dynamic Properties. It was noted above that metMbCN reconstituted with hemin **4** in the propionate orientation as in B (but not as in A) of Figure 1 exhibited anomalous line broadening for both the horse and sperm whale protein, with the effect larger for the former protein, and that the protein complexes with hemins **2** and **3** exhibited similar line broadening in horse but not sperm whale Mb, but again only when the sole propionate occupied position *f* as in B of Figure 1. Since the T_1s are the same for the two orientations of hemin **4** in sperm whale metMbCN (Table I), the anomalous line width, Δ, of peaks M_i must originate from a T_2 or chemical exchange process.

The absence of exchange processes for the isomer with the propionate oriented as in A (isomer A) of Figure 1 (peaks m_i) is evidenced by the straight line (solid line in Figure 7) with small positive slope for the plot of ln (Δ) versus reciprocal temperature, as found in native metMbCN.[26] In isomer B (with orientation as in B of Figure 1), the ln (Δ) versus T^{-1} plot approaches the behavior expected in the absence of exchange only at the lowest temperature (dotted line). As the temperature is raised, the line width increases dramatically, indicative of chemical exchange in the slow-exchange limit. However, it is clear that the component with which exchange is occurring is not isomer A, since its line widths are normal. The observed line-width phenomenon for peaks M_i, however, is consistent[34] with exchange between isomer B (with population p_B) and some undetected isomer C* (with population p_{C^*}), where the population of C* is minute, i.e., $p_B \gg p_{C^*}$. Under these circumstances, the ratio of exchange broadening of lines for isomer C* to that of B would be p_B/p_{C^*}, and with the already large line width for isomer B, the small intensity and excessive line width would render the peaks of isomer C* undetectable under experimentally accessible conditions. At the lowest temperature we fail to resolve the third set of peaks for isomer C*. The isomer B peaks still exhibit some exchange broadening at 5 °C, indicating that even under optimal attainable conditions, the peaks of isomer C* are both small and broad.

The case of two-site exchange, $B \rightleftarrows C^*$, between two highly differentially populated sites, $p_B \gg p_{C^*}$, has been treated in detail,[34] based on the characteristics of the generally only observed dominant B signal. As the interconversion rate increases, the B peak broadens, reaches a maximum width, Δ_{max}, and shifts by an amount $p_{C^*}\delta\nu$, where $\delta\nu$ is the shift difference of the B and C* environments, and then becomes narrower again. If p_{C^*} is small enough, this shift, $p_{C^*}\delta\nu$, may be negligible. The line-width data for the B isomer of hemin **4** in sperm whale metMbCN, as shown in both the spectra in Figure 2 and the line-width plot for M_a in Figure 7, are clearly consistent with this scenario, with the maximum line width observed at ~30 °C. This Δ_{max} has been shown to obey the relation:[34]

$$\Delta_{max} = p_{C^*}\delta\nu \quad (2)$$

which can be converted to the $B \rightarrow C^*$ rate, k_{BC^*}, via

$$k_{BC^*} = 2\pi\Delta_{max} \quad (3)$$

The observed Δ_{max} ~270 Hz at 30 °C yields $k_{BC^*} \sim 10^3$ s^{-1} for hemin **4** in sperm whale metMbCN. A comparison of the ^{1}H NMR spectra of sperm whale metMbCN reconstituted with hemin **4** recorded at 360 and 500 MHz exhibited a difference in the relative heights of the methyl peaks m_i and M_i for the same complex (not shown). While the spectral overlap precluded sufficiently quantitative determination of the line widths, it appeared that the narrow set of lines, m_i, had unchanged line widths,

(33) Woodward, C. K.; Hilton, B. D. *Annu. Rev. Biophys. Bioeng.* **1979**, *8*, 99–127.

(34) Sandström, J. *Dynamic NMR Spectroscopy*; Academic Press: New York, 1981; Chapter 6.

Table III. Site Interconversion and Predicted Chemical Shift Changes for Different Heme Rotational Variants of Isomer B

	isomer C		isomer E		isomer D	
site	new site	$\delta\nu^b$	new site	$\delta\nu^b$	new site	$\delta\nu^b$
a →	c	16	g	14	e	3
b →	d	11	h	8	f	2
d →	f	13	b	11	h	3
e →	g	17	c	19	a	3
f →	h	8	d	10	b	3

[a] The potential isomers C, D, and E have propionate locations as shown in C, D, and E, respectively, of Figure 1. [b] The chemical shift difference, in ppm, upon the specified site interconversion, are obtained from the mean values as shown in F of Figure 4.

indicating that the broader set, M_i, must experience some field-dependent line broadening to account for the reduced apparent heights, as predicted by eq 2, since $\delta\nu$ is proportional to field. The line widths for peak M_i for the horse metMbCN complex of hemin **4** increase even more dramatically than for the sperm whale protein, with several peaks becoming undetectable at 35 °C (D in Figure 4); hence temperature effects on line width could not be quantitated at high temperatures.

A clue as to the identity of the elusive, weakly populated third heme orientation corresponding to isomer C* can be derived from the qualitative pattern of the exchange broadening among the five resolved or partially resolved M_i resonances for isomer B. At 30 °C, the sperm whale metMbCN complex indicates the relative methyl line widths (as reflected qualitatively by the inverse of their relative heights) are $(M_a, M_c, M_d) > M_b > M_h$ (Figure 2). For a given dynamic process, eq 2 dictates[34] that the relative line widths parallel the differences in the isomer B and C* chemical shifts for each methyl, $\delta\nu_i$. The rapid B → C* interconversion and the absence of line broadening for peaks m_i of isomer A preclude a rotation about a meso–iron–meso axis,[11,12] which generally occurs at rates $\sim 10^4 - 10^5$ slower. The potentially more rapid rotational "hopping" about the pseudo-4-fold axis[35] would yield the isomers C–E of Figure 1 by a series of 90° rotations about the intact iron–His bond solely for isomer B. The changes in chemical shifts predicted upon converting isomer B to isomers D–E can be estimated from the empirical shift correlation with position in the protein matrix as given in F of Figure 1, and lead to $\delta\nu$'s as listed in Table III. Clearly, the relative shifts for the B → D conversion predict negligible differences for various methyls, contrary to observation, and the small shift changes could not account for the excessive broadening observed for the horse Mb complex. Both the B → C and B → E conversion correctly predict the larger line widths for M_c and M_a, but the case B → C agrees better in predicting the observed smallest line width effect on M_h. Hence we attribute the minor isomer C* in dynamic equilibrium with isomer B to that depicted in C of Figure 1. This orientation could have been anticipated as the most likely candidate based on the fact that the positions in isomers D and E would place the polar propionate side chain into the relatively nonpolar interior.

It is noted that the pattern of M_i line broadening of isomer B of horse metMbCN reconstituted with hemin **4** is essentially the same as for the sperm whale protein. Based on nearly identical shifts to the sperm whale proteins for both the A and B isomers (Table I), the shifts for isomer C can also be expected to be the same. Hence the larger line width for the M_i peak in the horse than sperm whale protein indicates that the B → C conversion rate is faster than for the sperm whale protein. Moreover, the anomalous line broadening for the M_i peaks of the B isomer for horse metMbCN reconstituted with hemins **2** and **3** most likely arises from the same dynamic process. The smaller excess line width for hemins **2** and **3** (Figure 6) relative to **4** (Figure 3) dictates that the B → C process is slower when the vinyls are present. Vinyls have been noted to result in slower heme reorientation in previous studies.[11] The slower B → C rate in sperm whale versus horse metMbCN complex of hemin **4** also rationalizes the negligible line broadening previously observed[12] for the sperm whale metMbCN complexes of hemins **2** and **3**. The faster B → C conversion rate of horse relative to sperm whale Mb for all three hemins **2**, **3**, and **4** likely reflects the weaker salt bridge to CD3 for Lys relative to Arg, as detected above in the preferences between isomers A and B.

Acknowledgment. This research was supported by grants from the National Science Foundation, DMB-87-03611, and the National Institutes of Health, HL-22252.

(35) Neya, S.; Funasaki, N. *Biochim. Biophys. Acta* **1988**, *952*, 150–157.